Measurement of $\sigma * BR(W + \gamma)$ and $\sigma * BR(Z + \gamma)$ at CDF

The CDF Collaboration[1]
Doug Benjamin
Tufts University
Medford, MA 02155 USA

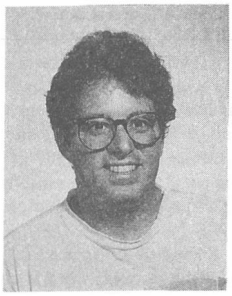

Abstract

We have measured the cross section × branching ratio for $W + \gamma$ and $Z + \gamma$ in the electron and muon channels using the W and Z data samples from the CDF '88-'89 collider run, in $4.05 \pm 0.28\ pb^{-1}$ ($3.54 \pm 0.24\ pb^{-1}$) of electron (muon) data. For central photons with $E_T^\gamma > 5.0\ GeV$ and $\Delta R_{\ell\gamma} > 0.7$, we observe 8 (5) electron (muon) $W\gamma$ candidates and 2 (2) electron (muon) $Z\gamma$ candidates. From these events, we measure $\sigma * BR(W\gamma) = 17.9^{+11.1}_{-10.7}\ (stat + syst)\ pb$ and $\sigma * BR(Z\gamma) = 9.2^{+5.2}_{-5.1}\ (stat + syst)\ pb$ for the $e + \mu$ combined sample. From the $W\gamma$ cross section × branching ratio measurement, we obtain limits on anomalous $WW\gamma$ couplings of the $-6.5 < \Delta\kappa < +6.9$ ($\lambda = 0$) and $-3.1 < \lambda < +3.1$ ($\Delta\kappa = 0$) at the 95% CL.

1 Introduction

The Standard Model (SM) unifies the electromagnetic and weak interactions into a single interaction described by the gauge group $SU(2)_L \otimes U(1)_Y$. This theory predicts the existence of the $\mathbf{W^{\pm}}$ vector bosons as carriers of the charged weak currents and two neutral vector bosons as carriers of the neutral currents, the γ and the Z^0. The measurement of W and Z production cross sections and decay properties at $\sqrt{s} = 1.8\ TeV$ $\bar{\text{p}}$-p collisions tests the strength and the nature of the couplings of gauge boson to quarks and leptons. The measurement of the $W^{\pm}\gamma$ and $Z^0\gamma$ production cross sections and final-state kinematics provides an experimental test of the trilinear gauge boson couplings and also simultaneously yields new information on static electromagnetic multipole moments of the W boson[2,3].

2 Data Samples

The $W\gamma$ and $Z\gamma$ candidate events were obtained from the 1988-89 inclusive W and Z data sets, which were used for the electron and muon W and Z cross-section $\times$ branching ratio measurements and the electron and muon W/Z cross-section ratios [4]. A total of $\int \mathcal{L}_e dt = 4.05 \pm 0.28$ pb^{-1} of electron data and $\int \mathcal{L}_\mu dt = 3.54 \pm 0.24$ pb^{-1} of muon data were collected this run[4].

Each of the inclusive W and Z data sets require at least one well measured, isolated, high transverse momentum (P_T) lepton in a good fiducial region of the central electromagnetic calorimeter (CEM) for electrons and central muon chambers (CMU) for muons. *Additionally*, W events must contain a neutrino whose signature is large missing transverse energy ($\not\!\!E_T > 20\ GeV$). Z^0 events require a second lepton and have a dilepton mass in a window centered on the Z^0 mass. The Z events are removed from the W data sample. The precise description of the W and Z selection in the electron and muon channels can be found in [4].

The electron and muon $W\gamma$ and $Z\gamma$ sub-datasets are formed by requiring an additional isolated well-measured photon passing the following criteria: the EM cluster have $|\eta_\gamma| < 1.1$; be within a good fiducial region of CEM calorimeter; the extra transverse energy deposited in a cone $\Delta R = 0.4$ centered on the photon, but not *including* the photon: $E_T^{\text{cone}} - E_T^{\text{photon}} < 2.0\ GeV$ (*Calorimeter isolation*); the sum of the transverse momentum due to charged tracks within a cone of $\Delta R = 0.4$ centered on the photon: $\sum P_T^{\text{cone}}(\Delta R = 0.4) < 2.0\ GeV$ (*tracking isolation*); no three dimensional tracks pointing at the EM cluster; electromagnetic energy fraction of the EM cluster be consistent with photons; transverse shower shape in the CEM calorimeter towers be consistent with testbeam photons; transverse shower shape in the proportional chamber at EM shower maximum (CES) be consistent with photons in both views $r - \phi$ and $z(\eta)$; no other clusters of energy in the CES detector (within the CEM cluster) in either the z or $r - \phi$ views with E > 1.0 GeV; and an angular separation between the W/Z decay lepton(s) and the photon $\Delta R_{\ell\gamma} > 0.7$. The isolation cuts are designed to reduce the QCD background. Requiring no second CES cluster further suppresses the π^0 and other multi-photon backgrounds. The $\Delta R_{\ell\gamma}$ cut is designed to suppress the contribution of radiative decay (as opposed to W/Z γ production) in the signal. The overall efficency for finding CEM photons was determined to be $\epsilon_\gamma = 80 \pm 1\%$. We observe 8(5) electron (muon) $W\gamma$ and 2(2) electron (muon) $Z\gamma$ candidates.

3 Backgrounds

The largest photon background in the $W\gamma$ and $Z\gamma$ signal is due to the combination of a QCD jet faking a photon and to a lesser extent prompt isolated photons due to initial/final state radiation (quark QED bremsstrahlung). The photon backgrounds due to QCD jets in the inclusive electron and muon W and Z data samples were determined using a multi-jet data sample. This QCD sample required two high E_T jets (*leading*) kinematically similiar to jets from hadronic $W(Z)$ decay. The other ($non - leading$) jets in the event were used to measure the fragmentation rate. The non-leading jets were required to pass all photon selection cuts. The probability of jet to pass all γ cuts is $\approx$ 0.2%.

As a cross-check on the determination of QCD backgrounds for each of the four W/Z data samples, VECBOS [5] + Herwig MC + CDF detector simulation was used to generate W/Z + n jets ($njets \leq 2\ jets$). These events were then required to pass all $W\gamma$ /$Z\gamma$ cuts. The systematic uncertainty on the QCD background for each of the four channels is defined as the difference between the QCD background derived from the QCD data sample and the the QCD background derived from the W/Z + jets Monte Carlo simulation. Other backgrounds to $W\gamma$ and $Z\gamma$ physics include Z + γ and Z + $jet - faking\ photon$ where one of the leptons from Z^0 decay is not detected and the Z is misidentified as a W. The proceses $(W \rightarrow \tau\nu_\tau) + \gamma$ and $(W \rightarrow \tau\nu_\tau)$ + Jet can also contribute to the background in the electron and muon $W\gamma$ data samples when the τ decays to an electron or muon, respectively. The corresponding processes $(Z \rightarrow \tau^+\tau^-) + \gamma$ and $(Z \rightarrow \tau^+\tau^-))$ + Jet contribute negligibly to the background in the electron and muon $Z\gamma$ data samples. The Drell-Yan contributions to $Z\gamma$ in the $M_{\ell^+\ell^-}$ mass window used is also small ($<$ 3 %). Table 1 contains a summary of the backgrounds for $W\gamma$ / $Z\gamma$.

Table 1 - Backgrounds for $W\gamma$ and $Z\gamma$

Channel	N^V_{QCD}	$N^{Z\gamma} + N^{Z\gamma}_{QCD}$	N^{Wre}
$W(e\nu)\gamma$	$3.57 \pm 0.81 \pm 1.47$	$0.14 \pm 0.02 \pm 0.07$	0.11 ± 0.01
$W(\mu\nu)\gamma$	$1.87 \pm 0.42 \pm 0.84$	$0.44 \pm 0.07 \pm 0.12$	0.06 ± 0.01
$Z(e^+e^-)\gamma$	$0.30 \pm 0.07 \pm 0.14$	—	—
$Z(\mu^+\mu^-)\gamma$	$0.11 \pm 0.03 \pm 0.04$	—	—

4 Determination of $\sigma * BR(W + \gamma)$ and $\sigma * BR(Z + \gamma)$

The $W\gamma$ and $Z\gamma$ Monte Carlo programs developed by Ulrich Baur[6] were used to generate electron,muon and tau $W\gamma$ and $Z\gamma$ data samples. This data coupled with a "fast" and very detailed MC detector simulation was used to determine geometric and kinematic acceptances. In addition, $W\gamma$ and $Z\gamma$ cross sections were obtained for events passing the W and Z boson event selection, the $\Delta R_{\ell-\gamma} > 0.7$ and $E_T^\gamma > 5.0\ GeV$ photon cuts. This MC data was used to make predictions on the expected number of $W\gamma$ and $Z\gamma$ events in the CDF electron and muon $W\gamma$ and $Z\gamma$ data samples, entering all relevant electron, muon and photon *efficiencies*.

The experimental results for the cross-section $\times$ branching ratio in the electron/muon channels were determined from

$$\sigma_V \cdot B(V+\gamma) = \frac{\mathcal{N}^{V\gamma}_{observed} - \sum \mathcal{N}^{V\gamma}_{background}}{A_{V\gamma} \cdot \epsilon_{V\gamma} \cdot \int \mathcal{L}_\ell dt} = \frac{\mathcal{N}^{V\gamma}_{signal}}{A_{V\gamma} \cdot \epsilon_{V\gamma} \cdot \int \mathcal{L}_\ell dt} \tag{1}$$

where $V = W$ or Z, $A_{V\gamma} \cdot \epsilon_{V\gamma}$ is the product of the acceptances $\times$ efficency factors for detecting $V\gamma$ events and $\ell = e$ or μ.

We can derive the *combined* electron and muon $\sigma \cdot BR(W + \gamma)$ and $\sigma \cdot BR(Z + \gamma)$ using a method similar to that used for determining the $\sigma \cdot BR(V + \gamma)$ for the individual channels. If we assume lepton universality, the combined $\sigma \cdot BR(V + \gamma)$ can be written as:

$$\sigma * BR(V+\gamma) = \frac{N_e^{signal} + N_\mu^{signal}}{\int \mathcal{L}_e dt \cdot A_e^{V\gamma} \cdot \epsilon_e^{V\gamma} + \int \mathcal{L}_\mu dt \cdot A_\mu^{V\gamma} \cdot \epsilon_\mu^{V\gamma}} \tag{2}$$

We see in table 2 that the cross section $\times$ branching ratio for both channels and the combined results of $W\gamma$ and $Z\gamma$ are good agreement with the SM predictions.

Table 2 - $\sigma * BR$ for $W\gamma$ and $Z\gamma$

Process	e (pb)	μ	e + μ	SM
$\sigma * BR(W\gamma)$	$17.0^{+13.7}_{-13.4}\ (stat + syst)$	$19.4^{+18.3}_{-17.9}$	$17.9^{+11.1}_{-10.7}$	$19.0\ ^{+3.3}_{-0.9}$
$\sigma * BR(Z\gamma)$	$6.8\ ^{+5.7}_{-5.7}\ (stat + syst)$	$13.6^{+10.3}_{-10.1}$	$9.2\ ^{+5.2}_{-5.1}$	$4.7\ ^{+0.7}_{+0.2}$

5 Limits on Anomalous Couplings for $W\gamma$

The Baur $W\gamma$ MC coupled with a fast detector simulation was used to obtain 68.3%, 90% and 95% CL upper limits for $\Delta\kappa = \kappa - 1$ and λ parameters on a grid of 80 $\Delta\kappa$ and λ points. The MC $\sigma \cdot BR(W\gamma)$ data is then fit using MINUIT to obtain a 3-dimensional description of the $\sigma * BR(W\gamma)$ cross section surface in the $\Delta\kappa - \lambda$ plane. The parametrization of the fit is of the following form:

$$\sigma(\Delta\kappa, \lambda) = \sigma_{SM} + a\Delta\kappa + b\Delta\kappa^2 + c\lambda + d\lambda^2 + e\Delta\kappa\lambda \quad (3)$$

No higher-order terms in $\Delta\kappa$, λ are needed, since the invariant amplitude $\mathcal{M}$ containing the anomalous contributions to the $W\gamma$ process is *linear* in the anomalous parameters κ and λ; the term $e\Delta\kappa\lambda$ is due to the interference between the various amplitudes associated with the $W\gamma$ process. Figure 1 shows the projection of the $W\gamma$ cross section on the κ or λ axis. The central value of the combined $e+\mu$ $\sigma * BR(W+\gamma)$ experimental result is shown as a horizontal solid line, the $\pm 1\sigma$ (stat+syst) (68% double-side CL) are shown as horizontal dashed lines; the 90% and 95% single sided CL are also shown. Figure 2 contains the 68.3%, 90% and 95% single sided CL contours in the $\Delta\kappa - \lambda$ for the combined $e+\mu$ $W\gamma$ results. Note, the displacement of the location of the minimum of the $\sigma * BR(W+\gamma)$ cross section relative to the SM value.

The UA2 experiment recently published limits on κ and λ from an analysis of 13 pb^{-1} of electron $W\gamma$ data using two different methods: the first method is equivalent to ours, comparing the number of signal events to the number of predicted events, and the second method obtained limits by fitting the P_T^γ spectrum[7]. Our results are comparable with the UA2 results; the results from both experiments are summarized in Table 3.

Table 3: CDF *vs* UA2 Comparison of $\Delta\kappa$ – λ Limits

Parameter	CL Range	CDF $e+\mu$ Limits	UA2 $\sigma * B$	UA2 P_T^γ Method
$\Delta\kappa$	68.3% DS	$0.0^{+4.7}_{-4.2}(stat) \pm 0.6(syst)$	$0.0^{+4.6}_{-4.2}(stat) \pm 1.0(syst)$	$0.0^{+2.6}_{-2.2}$ $(stat)$
	68.3% SS	$-3.2 < \Delta\kappa < +3.7$	–	–
$(\lambda = 0)$	90.0% SS	$-5.7 < \Delta\kappa < +6.1$	–	–
	95.0% SS	$-6.5 < \Delta\kappa < +7.0$	$-6.3 < \Delta\kappa < +6.9$	$-4.5 < \Delta\kappa < +4.9$
λ	68.3% DS	$0.0^{+2.0}_{-2.0}(stat) \pm 0.3(syst)$	$0.0^{+2.9}_{-2.9}(stat) \pm 0.7(syst)$	$0.0^{+1.7}_{-1.8}$ $(stat)$
	68.3% SS	$-1.6 < \lambda < +1.6$	–	–
$(\Delta\kappa = 0)$	90.0% SS	$-2.7 < \lambda < +2.7$	–	–
	95.0% SS	$-3.1 < \lambda < +3.1$	$-4.4 < \lambda < +4.4$	$-3.6 < \lambda < +3.5$

Since the W boson magnetic dipole moment $\mu_W = \frac{e}{2M_W}(2+\Delta\kappa+\lambda)$, electric quadrupole moment $Q_W = -\frac{e}{M_W^2}(1+\Delta\kappa-\lambda)$ and the W boson mean-squared charge radius $< R_W >^2 = \frac{1}{M_W^2}(1+\Delta\kappa+\lambda)$ are related to $\Delta\kappa$ and λ, we can derive the limits on the EM moments. In the SM (at tree level): $\Delta\kappa = 1-\kappa = 0$, $\lambda = 0$; in the SM $\mu_W^\circ = \frac{e\hbar c}{2M_W c^2}$ and $Q_W^\circ = -e\left(\frac{\hbar c}{M_W c^2}\right)^2 = -e\lambda_W^2$ where λ_W is the (reduced) Compton wavelength fo the W boson. Table 4 summarizes the combined $e+\mu$ limits on the W electromagnetic moments μ_W and Q_W. Figure 3 shows the 68.3%, 90.0% and 95.0% single-sided CL contours in the $Q_W/Q_W^\circ - \mu_W/\mu_W^\circ$ plane for the combined $e+\mu$ results.

Table 4: CDF Limits on W Boson EM Moments

Parameter	CL Range	CDF $e+\mu$ Limits
μ_W/μ_W°	68.3% $DS\ CL$	$2.0\ ^{+3.2}_{-3.1}\ (stat)\ \pm\ 0.5\ (syst)\ =\ 2.0\ ^{+3.6}_{-3.6}\ (stat+syst)$
	68.3% $SS\ CL$	$-2.4\ <\ \mu_W/\mu_W^\circ - 2\ \equiv\ g_W - 2\ <\ +2.5$
$(Q_W/Q_W^\circ = 1)$	90.0% $SS\ CL$	$-4.2\ <\ \mu_W/\mu_W^\circ - 2\ \equiv\ g_W - 2\ <\ +4.2$
	95.0% $SS\ CL$	$-4.8\ <\ \mu_W/\mu_W^\circ - 2\ \equiv\ g_W - 2\ <\ +4.9$
Q_W/Q_W°	68.3% $DS\ CL$	$1.0\ ^{+4.9}_{-4.5}\ (stat)\ \pm\ 0.7\ (syst)\ =\ 1.0\ ^{+5.6}_{-5.2}\ (stat+syst)$
	68.3% $SS\ CL$	$-3.5\ <\ Q_W/Q_W^\circ - 1\ \equiv\ q_W - 1\ <\ +3.8$
$(\mu_W/\mu_W^\circ = 2)$	90.0% $SS\ CL$	$-6.1\ <\ Q_W/Q_W^\circ - 1\ \equiv\ q_W - 1\ <\ +6.4$
	95.0% $SS\ CL$	$-7.0\ <\ Q_W/Q_W^\circ - 1\ \equiv\ q_W - 1\ <\ +7.4$
$<R_W>^2/\lambda_W^2$	68.3% $DS\ CL$	$1.0\ ^{+3.2}_{-3.1}\ (stat)\ \pm\ 0.5\ (syst)\ =\ 1.0\ ^{+3.6}_{-3.6}\ (stat+syst)$
	68.3% $SS\ CL$	$-2.4\ <\ <R_W>^2/\lambda_W^2 - 1\ \equiv\ r_W^2 - 1\ <\ +2.5$
$(Q_W/Q_W^\circ = 1)$	90.0% $SS\ CL$	$-4.2\ <\ <R_W>^2/\lambda_W^2 - 1\ \equiv\ r_W^2 - 1\ <\ +4.2$
	95.0% $SS\ CL$	$-4.8\ <\ <R_W>^2/\lambda_W^2 - 1\ \equiv\ r_W^2 - 1\ <\ +4.9$

6 Acknowledgments

We thank the Fermilab staff and the technical staffs of the participating institutions for their vital contributions. This work was supported by the U. S. Department of Energy and National Science Foundation; the Italian Istituto Nazionale di Fisica Nucleare; the Ministry of Science, Culture, and Education of Japan; the Natural Sciences and Engineering Research Council of Canada; and the A. P. Sloan Foundation.

We are extremely grateful to U. Baur for his enormous help with the various aspects of his $W\gamma$ and $Z\gamma$ Monte Carlo programs. We deeply appreciate the many stimulating discussions we have had with him during the course of this analysis.

References

[1] The CDF colaboration consists of the following institutions: Argonne National Laboratory - Brandeis University - Istituto Nazionale di Fisica Nucleare, University of Bologna - University of California at Los Angeles - University of Chicago - Duke University - Fermi National Accelerator Laboratory - Laboratori Nazionali di Frascati, Istituto Nazionale di Fisica Nucleare - Harvard University - University of Illinois - Institute of Particle Physics, McGill University and University of Toronto - The Johns Hopkins University - National Laboratory for High Energy Physics (KEK) - Lawrence Berkeley Laboratory - Massachusetts Institute of Technology - University of Michigan - Michigan State University - University of New Mexico - Osaka City University - Universita di Padova, Instituto Nazionale di Fisica Nucleare, Sezione di Padova - University of Pennsylvania - University of Pittsburgh - Istituto Nazionale di Fisica Nucleare, University and Scuola Normale Superiore of Pisa - Purdue University - University of Rochester - Rockefeller University - Rutgers University - Superconducting Super Collider Laboratory - Texas A&M University - University of Tsukuba - Tufts University - University of Wisconsin - Yale University

[2] S.J. Brodsky, R.W. Brown, Phys. Rev. Lett. **49**, 966 (1982).

[3] R.W. Robinett, Phys. Rev. **D28**, 1185 (1983).

[4] F. Abe *et al*, Phys. Rev. Lett. **64**, 152 (1990); F. Abe *et al*, Phys. Rev. **D44**, 29 (1991); F. Abe *et al*, Phys. Rev. Lett. **69**, 28 (1992).

[5] F.A. Berends, H. Kuijf, B. Tausk, W.T. Giele, Nucl. Phys. **B357**, 32(1991)

[6] U. Baur, E. L. Berger, Phys Rev **D41**, 1476 (1990); U. Baur, E. L. Berger, to appear in Phys Rev **D** (1993), and FSU-HEP-921030.

[7] J. Alitti, *et al*, Phys. Lett. **B 277**, 194 (1992).

Fig1 – Combined $e+\mu$ $\sigma*BR(W^{\pm}\gamma)$

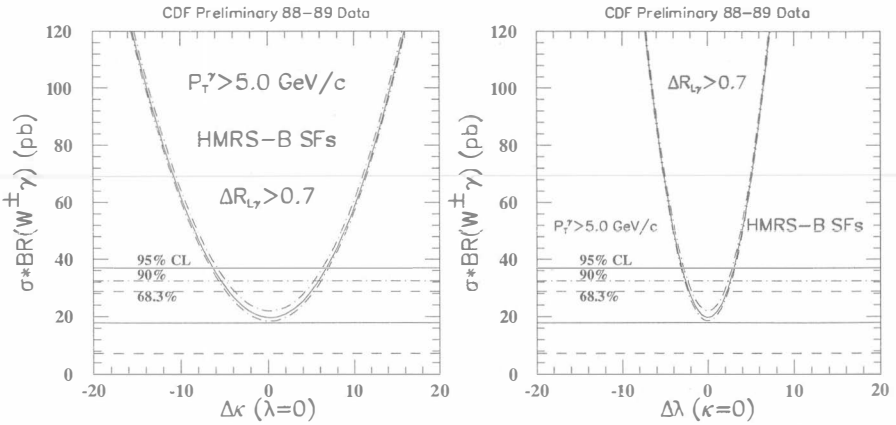

Fig 2 – Combined $e+\mu$ $W^{\pm}\gamma$ $\lambda-\Delta\kappa$

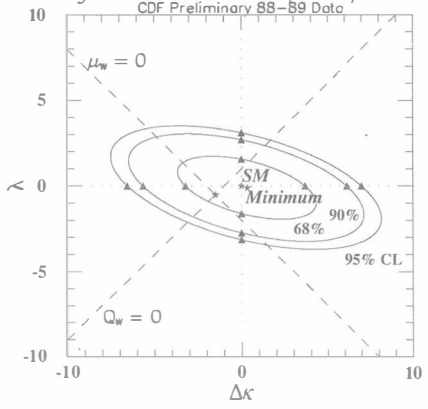

Fig 3 – Combined $e+\mu$ $W^{\pm}\gamma$ $Q_W-\mu_W$